Journal of Applied Polymer Science

Polymorphism and spherulite morphology of poly(1,4-butylene adipate)/organically-modified layered double hydroxide nanocomposites

Yi-An Chen, Yi-Tong Hang, Tzong-Ming Wu
Department of Materials Science and Engineering, National Chung Hsing University, 250 Kuo Kuang Road, Taichung, Taiwan, 402
Correspondence to: T.-M. Wu (E-mail: tmwu@dragon.nchu.edu.tw)

ABSTRACT: A novel biodegradable poly(1,4-butylene adipate)/organically-modified layered double hydroxide (PBA/m-LDH) nanocomposites are synthesized using the solution mixing process. The m-LDH is originally prepared with magnesium nitrate hexahydrote ($Mg(NO_3)_2$ $6H_2O$), aluminum nitrate-9-hydrate ($Al(NO_3)_3$ $9H_2O$), oleic acid, and sorbitol by a novel one-step co-precipitation method to intercalate the organo-modifier of oleic acid and sorbitol into the interlayer of LDH. The structure and morphology of the PBA/m-LDH nanocomposites are characterized using X-ray diffraction and transmission electron microscopy (TEM). It has been shown that the m-LDH is exfoliated and well distributed in PBA matrix. The effect of m-LDH on the polymorphic crystal and morphology of PBA at various crystallization temperatures (T_{cs}) would be investigated using WAXD and POM. Both data indicate that the addition of m-LDH can change the starting formation temperature of α-form crystals. © 2015 Wiley Periodicals, Inc. J. Appl. Polym. Sci. **2015**, *132*, 42526.

KEYWORDS: poly(1,4-butylene adipate); layered double hydroxide (LDH); nanocomposites; polymorphism

Received 12 March 2015; accepted 22 May 2015
DOI: 10.1002/app.42526

INTRODUCTION

Over the last several decades, biodegradable polymers, such as poly(1,4-butylene adipate) (PBA), polyhydroxyalkanoate (PHA), and poly(L-lactic acid) (PLLA), have attracted considerable attention due to their biodegradability for environmental and ecological advantages.[1] Among these biodegradable polymers, PBA is synthetic aliphatic and semicrystalline polyester and has been widely studied in academic researches. PBA contains two kinds of crystal forms designated as α- or β-form using various crystallization temperatures (T_{cs}).[2,3] The α-form crystal is found thermodynamically more stable than its β-form crystal because of high equilibrium melting temperature for the α-form crystals.[4] The morphology and polymorphic crystals of PBA stretched film were first studied by Minke and Blackwell.[2] According to their study, the α-form crystal contains a monoclinic unit cell with dimensions of a = 6.73 Å, b = 8.00 Å, c (fiber axis) = 14.20 Å, and β = 45.5°. The β-form crystal in PBA is characterized as an orthorhombic unit cell with dimensions of a = 5.05 Å, b = 7.36 Å, and c = 14.67 Å. Later, Gan *et al.*[4,5] found that a mixture of both α- and β-form crystals represented the morphology of ring-banded spherulites was formed between 28°C and 32°C, but the morphology of spherulites are ringless when crystallized at either above 32°C (α-form crystal) or lower than 28°C (β-form crystal). Therefore, the transformation of polymorphic crystal in PBA induced by different crystallization temperatures (T_{cs}) as well as by mixing with other polymers such as poly(phenyl methacrylate), poly(vinyl acetate), and poly(benzyl methacrylate) has been extensively studied.[6,7]

However, practical applications of PBA have been limited due to its low thermal stability, slow crystallization rate, and softness. In order to improve these properties, several investigations have added the inorganic fillers into the polymer matrix as reinforcement materials to enhance its hardness, thermal properties, and crystallization rate.[1,8] Reinforcing materials of numerous sizes and shapes have been well used in polymer composites.[8–10] Nevertheless, the effect of reinforcing materials on the polymorphism and morphology of PBA composites is not often mentioned among these reports. Layered double hydroxides (LDHs) are a kind of synthetic layered material that is similar to montmorillonite (MMT).[11] Compared to two-dimensional MMT, the two-dimensional LDHs contain high charge density and retain strong electrostatic interactions between hydroxide layers, which make the delamination of LDHs within polymer matrix more challenging.[12] To overcome the strong electrostatic interactions between hydroxide layers, organo-modifiers have been utilized to serve as delamination compounds of LDHs. More recently, organo-modifier with biocompatible and nontoxic properties, such as oleic acid,[13] γ-poly(glutamic acid),[14,15] and poly(lactide) with carboxyl end group (PLA–COOH),[16] have attracted considerable attention for their processing into the purpose for

© 2015 Wiley Periodicals, Inc.

biomedical and ecological applications. For example, the interlayer spacing of LDH is expanded using biocompatible γ-poly(-glutamic acid) as an organo-modifier.[14,15] The polymer chains would randomly distribute into the larger interlayer spacing of LDHs to form the polymer nanocomposites.

In this study, the biocompatible oleic acid and sorbitol are used as organo-modifier to prepare the organically-modified LDHs through one-step co-precipitation method (hereafter designated as m-LDH). The biodegradable PBA/m-LDH nanocomposites are fabricated using solution mixing process. The structure and morphology of the PBA/m-LDH nanocomposites were characterized using X-ray diffraction and transmission electron microscopy (TEM). The effect of m-LDH on the polymorphic crystal and morphology of PBA at various crystallization temperatures (T_{cs}) would be investigated using WAXD and POM.

EXPERIMENTAL

Materials and Preparation of PBA/m-LDH Nanocomposites

Sorbitol was purchased from Sigma-Aldrich Chemical Co. Magnesium nitrate hexahydrote ($Mg(NO_3)_2$ $6H_2O$), Aluminum nitrate-9-hydrate ($Al(NO_3)_3$ $9H_2O$), and sodium hydroxide were obtained from Fluka Chemical Co. Chloroform and oleic acid were purchased from Mallinckrodt Baker and Showa, respectively. All the chemicals were used without further purification.

Poly(1,4-butylene adipate) (PBA) purchased from Sigma-Aldrich Chemical Co. were purified by mixing PBA in chloroform solution and then precipitated at −10°C. The purified PBA was filtrated and then vacuum dried at 40°C for 72 h. The organo-modified magnesium/aluminum layered double hydroxides (hereafter designated as m-LDH) with molar ratio of Mg/Al = 2 were synthesized by the one-step co-precipitation method using biocompatible oleic acid and sorbitol as organo-modifier. The reactants of 0.02 mol $Mg(NO_3)_2$ $6H_2O$ and 0.01 mol $Al(NO_3)_3$ $9H_2O$ were dissolved in the 50 mL deionized water at room temperature. The organo-modifier of 0.012 mol oleic acid and sorbitol were individually dissolved in the 100 mL deionized water. Then, an aqueous solution containing reactant of $Mg(NO_3)_2$ $6H_2O$, $Al(NO_3)_3$ $9H_2O$, oleic acid, and sorbitol was vigorously stirred at 90°C for 24 h and simultaneously maintained pH value at 10.0 ± 0.2 by the dropwise addition of a 2*M* NaOH solution. All experimental processes were carried on under the nitrogen atmosphere. The obtained precipitates were filtered and washed three times systematically with ethanol, after which the remaining solids of LDH were freeze-dried and stored prior to further use. For comparison, the LDH prepared using the same co-precipitation method without oleic acid and sorbitol was obtained.

Various concentrations of PBA/m-LDH solution were prepared by solution mixing process in chloroform. The 0.1 g of PBA was dissolved in 10 mL chloroform and mechanically stirred for 24 h. Simultaneously, different weight ratios (0.1, 0.2, and 0.5 wt %) of m-LDH were added into 10 mL chloroform and ultrasonicated for 24 h to form the stable dispersion. The PBA/m-LDH nanocomposites were prepared by solution-direct intercalation process in chloroform solution and mechanically stirred for 6 h. The obtained solutions were poured into glass Petri dish and dried under vacuum at 40°C for 24 h. All fabricated PBA/m-LDH nanocomposites contained α-form crystal. In order to understand the structural behavior of PBA/m-LDH nanocomposites crystallized at various crystallization temperatures (T_{cs}) using the following WAXD experiments, the specimens were directly obtained from the following DSC isothermal crystallization experiments at T_{cs} in the range between 25°C and 44°C.

Characterization of PBA/m-LDH Nanocomposites

Wide-angle X-ray diffraction (WAXD) experiment equipped with Ni-filtered CuK_α radiation was recorded on a Bruker D8 Discover with a Scintillation counter detector. The scanning ranges of the specimens were collected from $2\theta = 1.1°$ to 40° with a scanning rate of 1°/min. Fourier transform infrared (FTIR) measurements were recorded on a Perkin-Elmer Spectrum One spectrometer in the transmission mode from 400 to 4000 cm^{-1} with an average of thirty spectra record of the samples. Transmission electron microscopy (TEM) performed on a Hitachi HF-2000 at 200 kV was used to characterize the distribution of m-LDH within the PBA/m-LDH nanocomposites. In order to observe the stacked LDH within the polymer matrix, the sample was immobilized in epoxy resin. Then, the resin embedded samples were microtomed at room temperature using a Reichert Ultracut ultramicrotome equipped with a diamond knife. The slices were collected on carbon-coated copper grid. Thermal analysis of PBA/m-LDH composites was analyzed using a PerkinElmer Pyris Diamond Differential scanning calorimeter (DSC). An indium standard was performed for calibration and all experiments were executed under a nitrogen atmosphere. The specimens weighed in the range of 5–6 mg were heated to pre-melting temperatures (T_{max}) of 150°C at a heating rate of 10°C/min and held for 5 min to erase the thermal history. Subsequently, the samples were rapidly cooled to the proposed crystallization temperatures (T_{cs}) at cooling rate of 100°C/min and held for a period of time until the crystallization was complete. The proposed T_{cs} were selected in the range between 36°C and 44°C. The exothermal traces were recorded for the data analysis. Polarized optical microscopy (POM) was performed with a Zeiss optical microscope equipped with crossed polarizers. The crystallization process of PBA/m-LDH composite was heated to melt at T_{max} =150°C for 5 min on a Mettler FP-82 hot stage to eliminate the previous thermal history. Subsequently, the samples were then cooled quickly to the proposed T_{cs}. POM data was recorded at the proposed T_{cs} for various times.

RESULTS AND DISCUSSION

Morphology of PBA/m-LDH Nanocomposites

The structures of LDH and m-LDH fabricated using the co-precipitation method was identified by X-ray diffraction method presented in Figure 1. The WAXD data of LDH reveals the strong diffraction peak at $2\theta = 10.6°$, which is corresponding to the interlayer distance of (003) plane.[17,18] By applying Bragg's equation, the interlayer spacing d_{003} of LDH was determined to be 8.3 Å. For the m-LDH, the position of the basal reflections of the modified LDH with oleic acid and sorbitol was shifted to

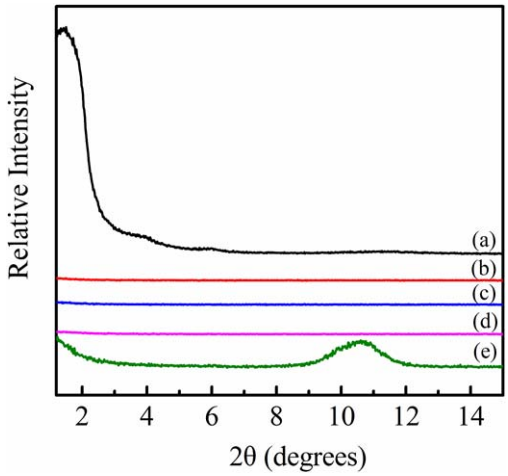

Figure 1. X-ray diffraction patterns of (a) m-LDH, (b) 0.1 wt % PBA/m-LDH, (c) 0.2 wt % PBA/m-LDH, (d) 0.5 wt % PBA/m-LDH nanocomposite, and (e) LDH. [Color figure can be viewed in the online issue, which is available at wileyonlinelibrary.com.]

smaller angle, indicating that the interlayer distance of the LDH was increased. The WAXD patterns of m-LDH showed the expanding layered structure with a sharp (003) diffraction peak at $2\theta=1.4°$, which reveals the interlayer spacing of 58.8 Å. These results suggest that the oleic acid and sorbitol were successfully exchanged and intercalated into the interlayer spacing of LDH.

The interlayer spacing of the fabricated PBA/m-LDH nanocomposites determined using X-ray diffraction is also shown in Figure 1. All WAXD patterns of PBA/m-LDH nanocomposites were represented by the disappearance of the (003) diffraction peaks corresponding to the LDH irrespective of the variation in the m-LDH content. This complete disappearance of the diffraction peaks could be due to the exfoliated structure, in which the gallery height of intercalated layers was large enough and the layer correlation was not detected by X-ray diffractometer. This result suggest that the molecular chains of PBA have been successfully inserted and well dispersed in them-LDH galleries even if the loading of m-LDH was as high as 0.5 wt %. Although WAXD provides a partial picture on the distribution of the nanofiller and disappearance of the diffraction peak corresponding to larger d-spacing or no regular periodicity of m-LDH, it does not always confirm the exfoliated nanocomposites, and a complete characterization of nanocomposite morphology requires microscopic investigation. Therefore, the dispersion of m-LDH enhanced with the molecular chain of PBA is supported by the TEM images shown in Figure 2. The TEM micrograph of embedded and cutted nanocomposite for 0.5 wt % PBA/m-LDH nanocomposite reveals that the original stacked lamellar structure of LDH can be modified to form the disorderly dispersed morphology in the PBA matrix. Both WAXD and TEM results demonstrate that most of the hydroxide layers are exfoliated and randomly dispersed in the PBA matrix. Therefore, the preparation of exfoliated PBA/m-LDH nanocomposites has been successfully by solution mixing process.

Polymorphism of PBA/m-LDH Nanocomposites

The polymorphism behavior and crystalline phase of PBA and PBA/m-LDH nanocomposites were investigated. Figure 3 illustrates the WAXD patterns of both neat PBA and the PBA/m-LDH nanocomposites, which were crystallized at various crystallization temperatures (T_{cs}). Peaks attributed to α- or β-crystal forms are clearly identified on the neat PBA diffractograms. When the crystallization temperature (T_{cs}) is 28°C, there are two diffraction peaks at $2\theta = 21.3°$ and 24.4°, labeled as peaks β_I and β_{II}, respectively. However, when the temperature is 32°C, two strong diffraction peaks at $2\theta = 21.8°$ and 22.5° (α_I and α_{II}) and a weak diffraction peak at $2\theta = 24.1°$ (α_{III}) are found to be located at entirely different positions with those at 28°C, suggesting that the crystal structure of PBA at 32°C is totally different from that at 28°C. These results indicate that the diffraction patterns of PBA melt-crystallized at 28°C correspond to β-crystal form, while those of crystallization temperature (T_{cs}) at 32°C correspond to α-crystal form. The crystal structures of PBA melt-crystallized at the temperature below 28°C or above 32°C are attributed to β-crystal or α-crystal form, respectively. The diffraction peaks of the PBA after melt-crystallized in the range between 28°C and 32°C consist of all the peaks except peak α_{III}, indicating the crystal structure is a mixture of α-crystal and β-crystal forms.

For PBA/m-LDH nanocomposites, various α- or β-crystal forms also presented in this figure are apparently dependent on T_{cs}

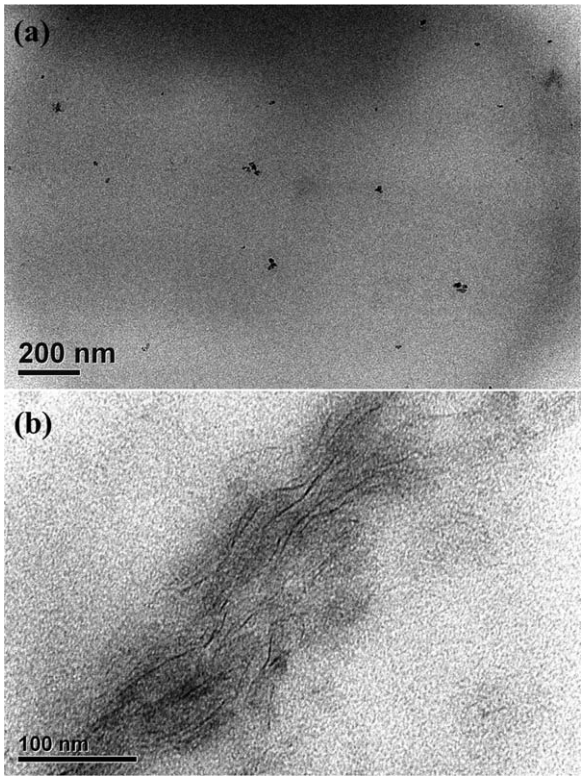

Figure 2. TEM micrographs of 0.5 wt % PBA/m-LDH.TEM micrograph obtained from the embedded and cutted 0.5 wt % PBA/m-LDH nanocomposite was shown in Figure 2(b).

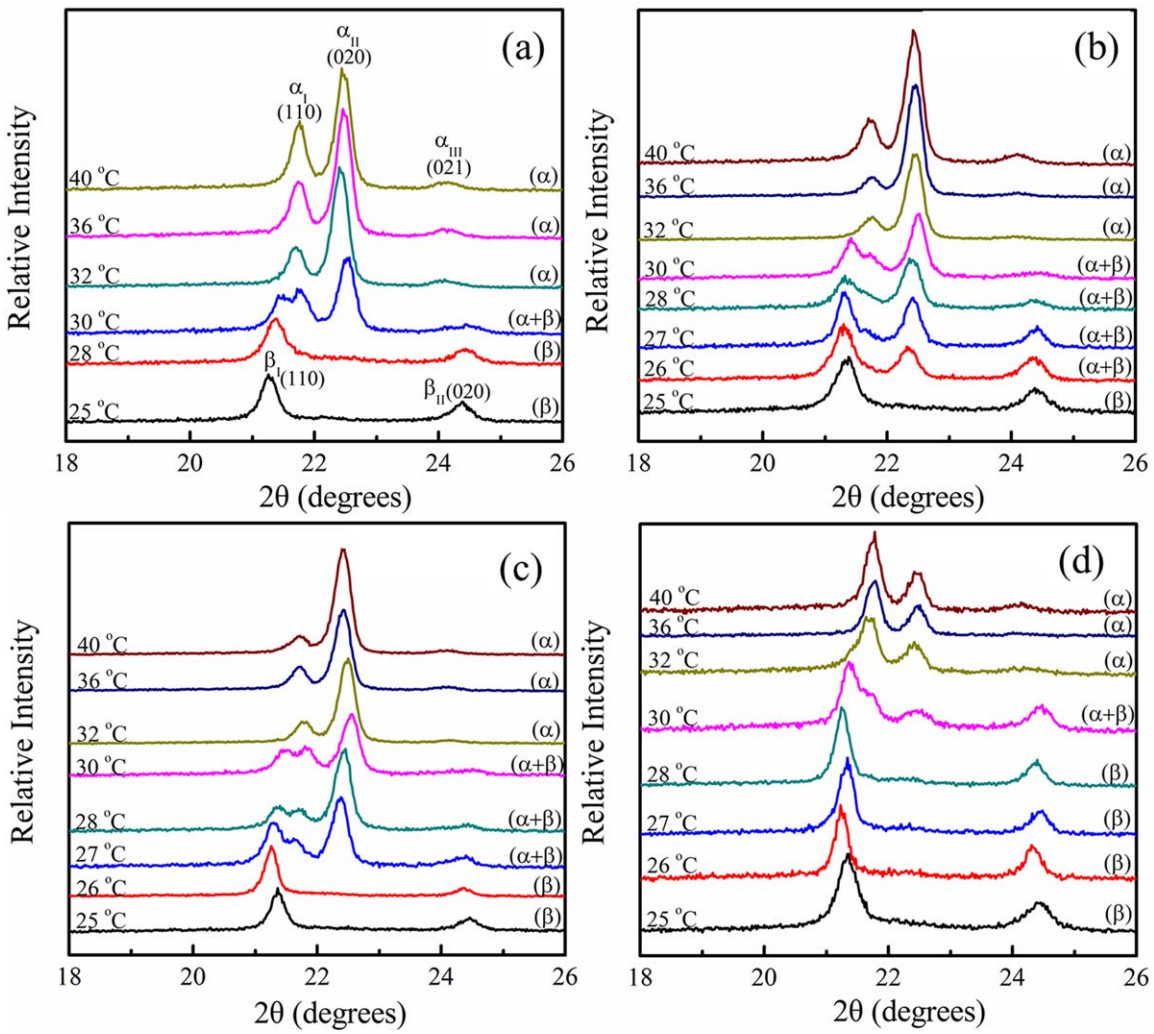

Figure 3. X-ray diffraction patterns of (a) PBA, (b) 0.1 wt % PBA/m-LDH, (c) 0.2 wt % PBA/m-LDH, and (d) 0.5 wt % PBA/m-LDH nanocomposites, crystallized at different temperatures as indicated on traces. [Color figure can be viewed in the online issue, which is available at wileyonlinelibrary.com.]

and the loading of m-LDH. All diffraction data of nanocomposites show two strong diffraction peaks (α_I and α_{II}) and a weak diffraction peak (α_{III}) when the crystallization temperature (T_{cs}) is $\geq$32°C, suggesting that the lower bound crystallization temperature (T_{cs}) of α-crystal form remains almost the same. For 0.1 wt % PBA/m-LDH nanocomposites, the upper bound crystallization temperature (T_{cs}) of β-crystal form is 25°C. The structure of PBA after melt-crystallized in the range between 25°C and 32°C reveals a mixture of α-crystal and β-crystal forms. As the loading of m-LDHB continuously increase to 0.2 wt % and 0.5 wt %, the upper bound crystallization temperature (T_{cs}) of β-crystal form is increased to 26°C and 28°C, respectively. These results demonstrate that the addition of m-LDH can change the formation temperature of α-form crystals.

The WAXD results have clearly shown the α- and β-crystal forms of PBA developed at different crystallization temperatures (T_{cs}). Other evidence was found from crystal morphology of PBA/m-LDH nanocomposites. Figure 4 shows the spherulite morphologies of PBA/m-LDH nanocomposites melt-crystallized at a temperature in the range from 25°C to 36°C using polarized optical microscopy (POM). The ranges of temperature were selected so that the spherulite patterns varied from being ringless at lower T_c to ring-banded, the back to ringless at higher T_c. For the PBA melt-crystallized at temperature range of 28–32°C, the morphologies of PBA are ring-banded spherulites. But ring-banded spherulites are presented in the PBA/m-LDH nanocomposites melt-crystallized at T_c= 28–32°C. This finding indicates that incorporation of m-LDH leads to the formation of α-form crystals at relatively lower T_c.

The simplified phase diagram obtained by WAXD and POM data is summarized in Figure 5. Apparently, for the PBA/m-LDH nanocomposites, the temperature range for polymorphism almost corresponds to ring-banded spherulites. Clearly, the addition of m-LDH has lots of influences on the formation of PBA polymorphic crystals. According to previous literature, the growth of metastable β-form crystals is kinetically preferential, and the addition of sorbitol can result in the reduction of surface free energy of nucleus.[19] It can be inferred that the

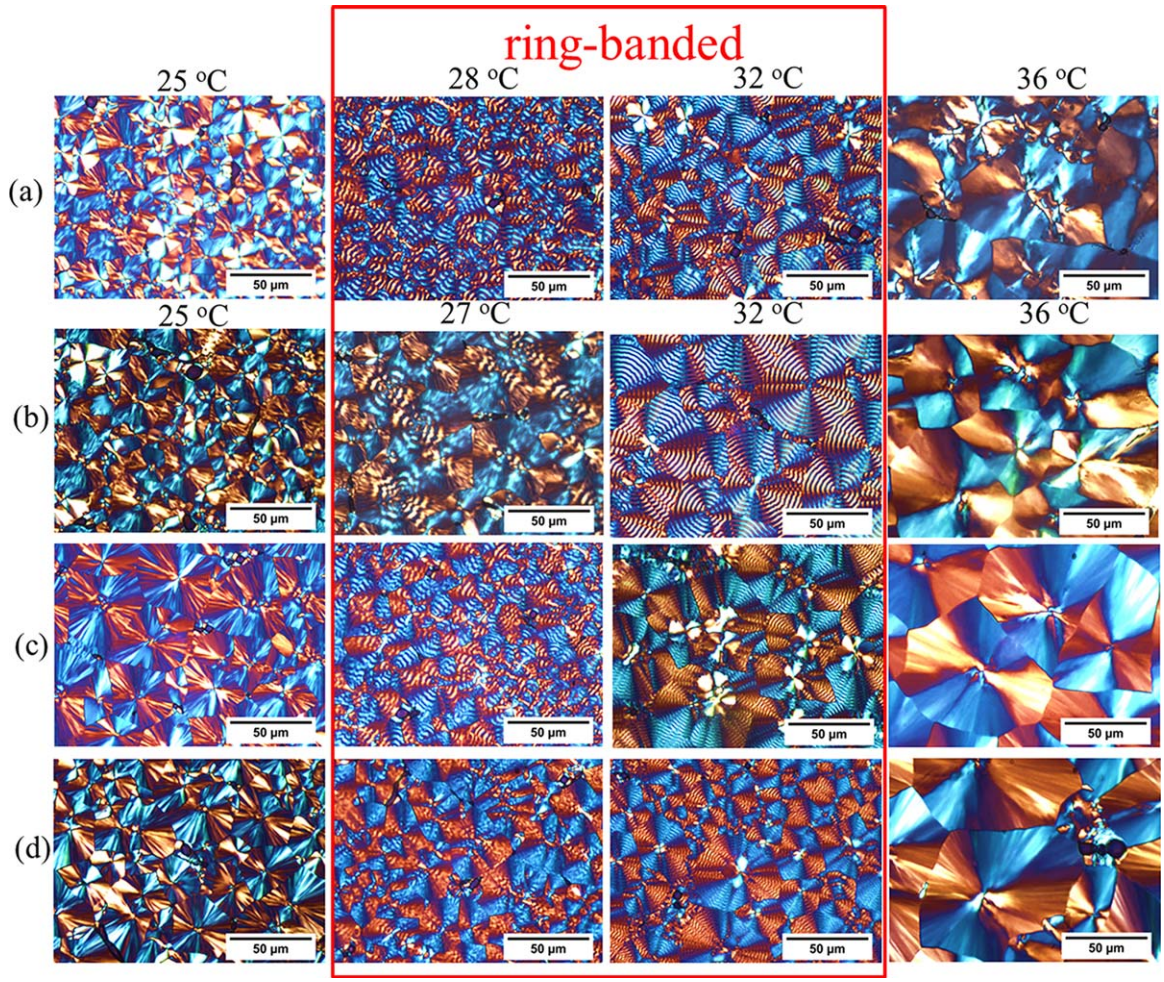

Figure 4. Optical micrographs of spherulitic morphology of (a) neat PBA, (b) 0.1 wt % PBA/m-LDH, (c) 0.2 wt % PBA/m-LDH, and (d) 0.5 wt % PBA/m-LDH nanocomposites after complete crystallization at different temperatures. [Color figure can be viewed in the online issue, which is available at wileyonlinelibrary.com.]

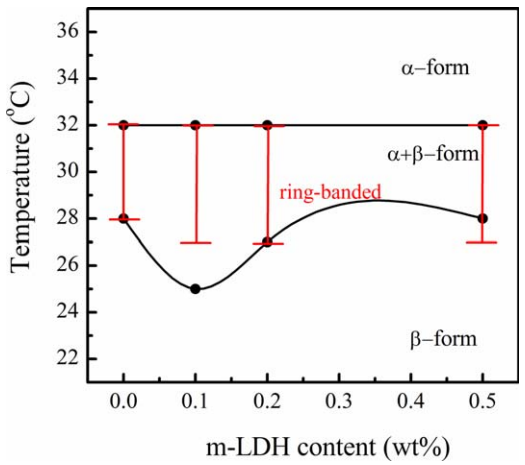

Figure 5. Temperature range of ring-banded spherulites and crystal types in PBA/m-LDH nanocomposites with different m-LDH content. (Red bars indicate T_c range for ring-banded spherulites). [Color figure can be viewed in the online issue, which is available at wileyonlinelibrary.com.]

reduction is strong enough, it is favorable for the formation of thermodynamically stable α-crystals, while the kinetically preferential growth of β-form crystals is no longer.[19]

Isothermal Crystallization of PBA and Its Nanocomposites

According to the data presented in Figure 5, the α-form crystals were developed at crystallization temperatures (T_{cs}) above 32°C. To avoid the influence of polymorphism on the crystallization behavior of PBA/m-LDH nanocomposites, the isothermal crystallization temperatures (T_{cs}) were chosen in the range of 36°C to 44°C. Therefore, the crystallization kinetics of neat PBA and its nanocomposites under isothermal conditions can be analyzed using the well-known Avrami equation, described as follows:[20,21]

$$1-X_t=\exp\left(-kt^n\right), \quad (1)$$

where the X_t is the relative crystallinity at different crystallization time t, k is the crystallization rate constant, and n is the Avrami exponent constant depending on the mechanism of nucleation and the form of crystal growth. To convert conveniently with the operation, eq. (1) can be transformed into

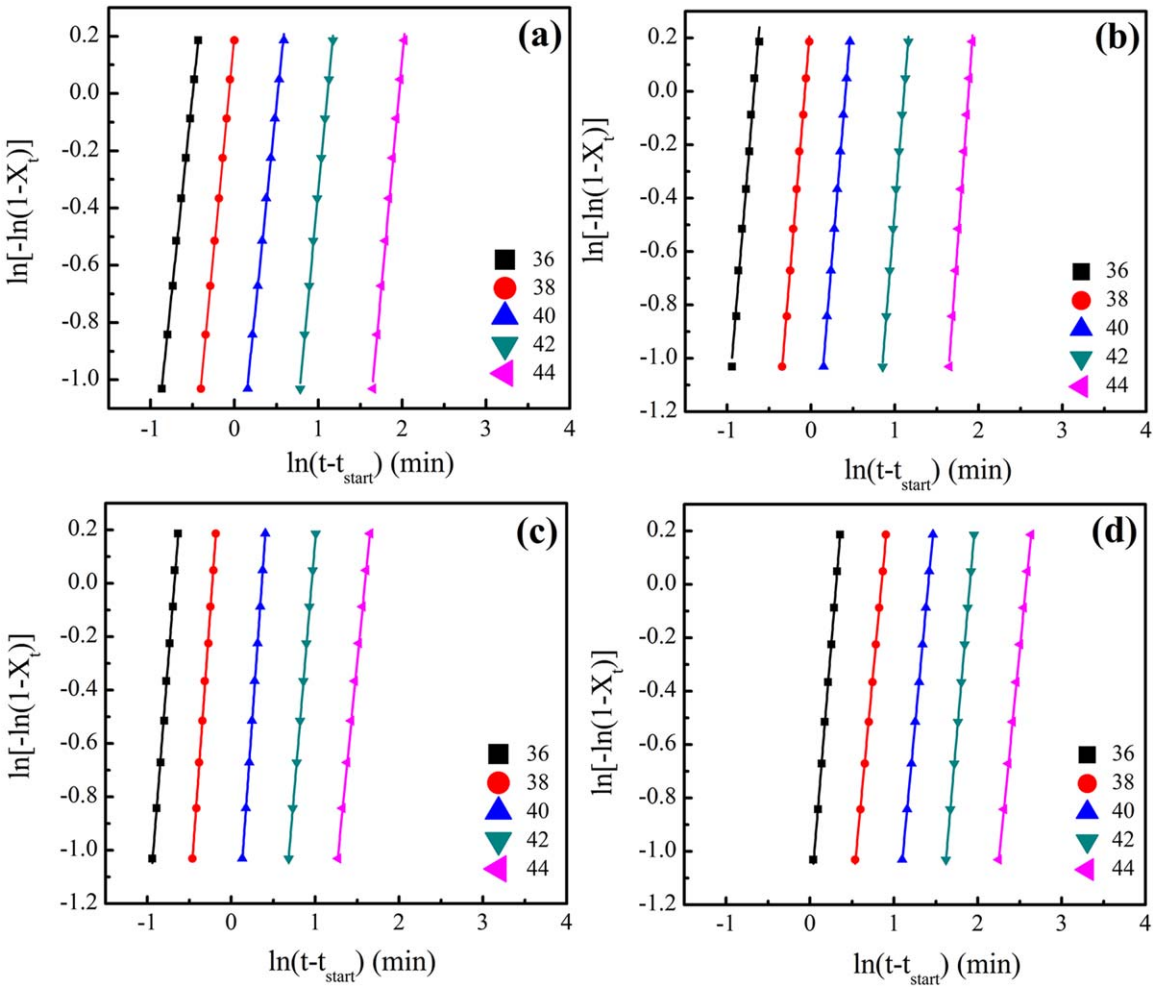

Figure 6. Avrami plots of (a) neat PBA, (b) 0.1 wt % PBA/m-LDH, (c) 0.2 wt % PBA/m-LDH, and (d) 0.5 wt % PBA/m-LDH nanocomposites. [Color figure can be viewed in the online issue, which is available at wileyonlinelibrary.com.]

$$\ln\left[-\ln\left(1-X_t\right)\right]=n\ln t+\ln k. \quad (2)$$

The time ($t_{1/2}$), at which half crystallization occurs, can be assumed. The values of $t_{1/2}$ are calculated from eq. (3):

$$t_{1/2}=\left(\frac{\ln 2}{k}\right)^{1/n}. \quad (3)$$

The Avrami plots of neat PBA and its nanocomposites are shown in Figure 6. All curves are almost parallel to each other, indicating that the crystallization mechanism of the PBA and its nanocomposites at different crystallization temperatures (T_{cs}) remains the same. The *n*- and *k*-values were obtained from the slopes and intercepts of the Avrami plots. For comparison, the obtained Avrami parameters are summarized in Table I. The *n*-values of neat PBA at given crystallization temperatures (T_{cs}) are between 2.78 and 3.23. The non-integral *n*-values that we obtained may occur because of the presence of crystalline branching and two-stage crystal growth during crystallization and a mixed growth and nucleation mechanism.[22] In general, a value of *n* close to 3 may represent an athermal nucleation process followed by a three-dimensional crystal growth and homogeneous nucleation mechanism. However, the obtained Avrami exponent *n* ranged from 3.18 to 4.46 for PBA/m-LDH nanocomposites at various crystallization temperatures (T_{cs}), suggesting a crystallization mode of heterogeneous nucleation for the isothermal melt crystallization process. Similar results have also been reported in the literature concerning the biodegradable polymers/nucleating agent composites.[23–25] In addition, due to the unit of k is min^{-n} and n is not constant in this work for all the samples at each T_c, it is not appropriate to compare the overall crystallization rate from the k values directly. Therefore, the crystallization half-life time ($t_{1/2}$), the time required to half completion of the final crystallinity of the samples, is employed to discuss crystallization kinetics of neat PBA and its nanocomposites and is also summarized in Table I. With the addition of 0.2 wt % m-LDH, the $t_{1/2}$ for crystallization of the PBA/m-LDH nanocomposite decreased compared with that of neat PBA. These results suggest that the addition of small amount m-LDH actually acts as effective nucleating agent and significantly speed up the crystallization rate of PBA. But the addition of 0.5 wt % m-LDH into PBA matrixes probably induced more physical barrier to reduce the mobility of polymer chains resulting in a bigger crystallization half-life time, which the $t_{1/2}$ values are bigger than that of 0.2 wt % PBA/m-LDH nanocomposites.

Table I. Kinetic Parameters of Neat PBA and PBA/m-LDH Nanocomposites Isothermally Melt Crystallized at T_c =36–44°C

Sample	T_c (°C)	n	k (min^{-n})	$t_{1/2}$ (min)
	36	2.78	4.0000	0.53
	38	3.04	1.2200	0.83
PBA	40	2.83	0.2330	1.47
	42	3.12	0.0215	2.69
	44	3.23	0.0018	6.35
	36	3.81	13.2768	0.46
	38	3.83	1.32745	0.84
0.1 wt % PBA/m-LDH	40	3.86	0.20422	1.37
	42	3.95	0.01239	2.77
	44	4.38	0.00261	6.03
	36	3.98	14.9340	0.46
	38	3.86	2.6849	0.73
0.2 wt % PBA/m-LDH	40	4.46	0.1982	1.32
	42	3.75	0.0275	2.36
	44	3.47	0.0064	4.39
	36	3.46	0.3019	1.25
	38	3.32	0.0591	2.10
0.5 wt % PBA/m-LDH	40	3.34	0.0090	3.67
	42	3.43	0.0010	6.07
	44	3.18	0.0003	11.73

CONCLUSIONS

WAXD diffraction pattern reveals that the interlayer spacing of the LDH and m-LDH are 8.3 Å and 58.8 Å, respectively. These results demonstrate that not only the possibility of the one-step co-precipitation for synthesizing m-LDH, but also the intercalated biocompatible oleic acid and sorbitol into the LDH gallery could further expand the interlayer spacing of LDH. Both WAXD and TEM results show that the majority of the hydroxide layers are exfoliated and randomly distributed in the PBA matrix. Therefore, the fabrication of exfoliated PBA/m-LDH nanocomposites has been successful by solution mixing process. With the loading of m-LDH, the starting formation temperature of α-form crystals of the PBA/m-LDH nanocomposites can be changed. The addition of m-LDH could also make considerable difference in terms of the crystallization behavior of nanocomposites.

ACKNOWLEDGMENTS

The financial support provided by National Science Council through the project NSC102–2212-E-005–093 is greatly appreciated.

REFERENCES

1. Zhao, Y.; Qiu, Z. *J. Nanosci. Nanotechno.* **2012**, *12*, 4067.
2. Minke, R.; Blackwell, J. *J. Macromol. Sci. Phys.* **1979**, *B16*, 407.
3. Minke, R.; Blackwell, J. *J. Macromol. Sci. Phys.* **1980**, *B18*, 233.
4. Gan, Z.; Kuwabara, K.; Abe, H.; Iwata, T.; Doi, Y. *Biomacromolecules* **2004**, *5*, 37.
5. Gan, Z.; Abe, H.; Doi, Y. *Macromol. Chem. Phys.* **2002**, *203*, 2369.
6. Wang, L. Y.; Lugito, G.; Woo, E. M.; Wang, Y. H. *Polymer* **2012**, *53*, 3815.
7. Lugito, G.; Woo, E. M. *Macromol. Chem. Phys.* **2014**, *213*, 2228.
8. Bordes, P.; Pollet, E.; Averous, L. *Prog. Polym. Sci.* **2009**, *34*, 125.
9. Ciardelli, F.; Coiai, S.; Passaglia, E.; Pucci, A.; Ruggeri, G. *Polym. Int.* **2008**, *57*, 805.
10. Pavlidoua, S.; Papaspyrides, C. D. *Prog. Polym. Sci.* **2008**, *33*, 1119.
11. Wang, D. Y.; Costa, F. R.; Vyalikh, A.; Leuteritz, A.; Scheler, U.; Jehnichen, D.; Wagenknecht, U.; Haussler, L.; Heinrich, G. *Chem. Mater.* **2009**, *21*, 4490.
12. O'Leary, S.; O'Hare, D.; Seeley, G. *Chem. Commun.* **2002**, *14*, 1506.
13. Ciou, C. Y.; Li, S. Y.; Wu, T. M. *Eur. Polym. J.* **2014**, *59*, 136.
14. Chiang, M. F.; Wu, T. M. *Appl. Clay Sci.* **2011**, *51*, 330.
15. Chiang, M. F.; Chen, E. C.; Wu, T. M. *Polym. Degrad. Stabil.* **2012**, *97*, 995.
16. Chiang, M. F.; Wu, T. M. *Compos. Sci. Technol.* **2010**, *70*, 110.
17. Chiang, M. F.; Chu, M. Z.; Wu, T. M. *Polym. Degrad. Stabil.* **2011**, *96*, 60.
18. Millange, F.; Walton, R. I.; O'Hare, D. *J. Mater. Chem.* **2000**, *10*, 1713.
19. Jiang, N.; Zhao, L.; Gan, Z. *Polym. Degrad. Stabil.* **2010**, *95*, 1045.
20. Avrami, M. *J. Chem. Phys.* **1940**, *8*, 212.
21. Avrami, M. *J. Chem. Phys.* **1941**, *9*, 177.
22. Alamo, R. G.; Mandelkern, L. *Macromolecules* **1991**, *24*, 6480.
23. Fornes, T. D.; Paul, D. R. *Polymer* **2003**, *44*, 3945.
24. Pei, A.; Zhou, Q.; Berglund, L. A. *Compos. Sci. Technol.* **2010**, *70*, 815.
25. Liao, R.; Yang, B.; Yu, W.; Zhou, C. *J. Appl. Polym. Sci.* **2007**, *104*, 310.